A New Water-Soluble, Self-Doping Conducting Polyaniline from Poly(*o*-aminobenzylphosphonic acid) and Its Sodium Salts: Synthesis and Characterization

H. S. O. Chan,*,† P. K. H. Ho,† S. C. Ng,*,† B. T. G. Tan,‡ and K. L. Tan‡

Contribution from the Departments of Chemistry and Physics, National University of Singapore, Kent Ridge, Singapore 0511, Republic of Singapore

Received March 27, 1995[⊗]

Abstract: Poly(*o*-aminobenzylphosphonic acid) and its sodium salts, made by progressive neutralization with NaOH, have been prepared and characterized. Both the hemisodium and monosodium salts are intrinsically self-doped and water-soluble in the conducting form. The key is to control the ionization of the excess acid functions on the polymer chains. XPS results suggest that the polymer is obtained directly in the 43% polyzwitterionic (i.e., self-doped) emeraldine form. The self-doped polymer does not exhibit any conductivity dependence on pH below 6, in marked contrast to the HCl-doped polyanilines. Our structurally well-defined polymer system displays only one set of redox activity over the potential range of −0.2 to 1.2 eV, alluding to the higher stability of the self-doped structure. This is unique and different from other polyaniline systems which show two sets of redox peaks. FTIR spectroscopy provides evidence for strong intra-chain hydrogen bonding while NMR studies conclude that protonated and unprotonated segments of the solvated monosodium polymer are distinct. The lower conductivity ($\sim 10^{-3}$ S cm^{-1}) obtained is attributed to the decrease in conjugation caused by the large steric effect of the bulky PO_3H_2 and a significant hydrogen bond interaction between $PO_2(OH)^-$ and $NH^{\bullet+}$ leading to significant charge-pinning. UV−vis data can be explained by a increased participation of the nitrogen wave function in the HOMO, and thereby the widening of the $\pi_B \rightarrow \pi_S$ band gap.

Introduction

Although the structure and organic chemistry were investigated by Green[1] and Willstatter[2] in the early 20th century, polymerization of aniline has received a great deal of attention only in the last 15 years or so because it was the first conducting polymer whose electronic properties could be reversibly controlled by both protonation and charge-transfer doping.[3] The ability to exist in various forms via acid/base treatment and oxidation/reduction, either chemically or electrochemically, has made polyaniline the most "tunable" of the conducting polymers. Polyaniline can be used as an electrode material,[4] in the fabrication of batteries,[5] in microelectronics,[6] and as electrochromic materials for making displays.[7]

It is now recognized that for some niche applications, intrinsically conducting polymer may only require conductivity in the region of 1×10^{-3} to 1×10^{-2} S cm^{-1}, e.g., when used as an antistatic agent,[8] as EMI shielding materials,[9] and as a host for enzyme entrapment in the construction of biosensors.[10] In many cases it is more important if the polyanilines were soluble and processable than if they were highly conductive. In the past few years much progress has been made to improve both areas through the preparation of novel aniline derivatives,[11] the post treatment of polyaniline such as sulfonation or incorporation of N-alkylsulfonic acid pendant groups,[12] the use of functional dopants,[13] the design of self-doping polymer,[14] the control of molecular weight,[15] the use of microemulsion polymerization technique,[16] and the polymerization of aniline monomers on a template such as a polymeric acid.[17]

Apart from the obvious drawbacks, such as poor solubility in common organic solvents and the inability to flow without

* Authors to whom correspondence should be sent.
† Department of Chemistry.
‡ Department of Physics.
⊗ Abstract published in *Advance ACS Abstracts*, August 1, 1995.

(1) Green, A. G.; Woodhead, A. E. *J. Chem. Soc.* **1910**, *97*, 2388; **1912**, *101*, 1117.
(2) Willstatter, R.; Moore, C. W. *Chem. Ber.* **1907**, *40*, 2665.
(3) (a) MacDiarmid, A. G.; Chiang, J. C.; Halpern, M.; Huang, W. S.; Mu, S. L.; Somasiri, N. L. D.; Wu, W.; Yaniger, S. I. *Mol. Cryst. Liq. Cryst.* **1985**, *121*, 173−180. (b) Huang, W. S.; Humphery, B. D.; MacDiarmid, A. G. *J. Chem. Soc., Faraday Trans.* **1986**, *82*, 2358. (c) MacDiarmid, A. G.; Chiang, J. C.; Richter, A. F.; Epstein, A. J. *Synth. Met.* **1987**, *18*, 285−290. (d) Naarman, H. *Adv. Mater.* **1990**, *2*, 345.
(4) Genies, E. M.; Hany, P.; Santier, C. J. *J. Appl. Electrochem.* **1988**, *18*, 285.
(5) Kaneko, M.; Nakamura, H. *J. Chem. Soc., Chem. Commun.* **1985**, 346.
(6) (a) Paul, E. W.; Ricco, A. J.; Wrighton, M. S. *J. Phys. Chem.* **1985**, *89*, 1441. (b) Huang, W. S.; Lecorre, M. A.; Tissier, M. *J. Vac. Sci. Technol.* **1991**, *B9*, 3428. (c) Chen, S. A.; Fang, Y. *Synth. Met.* **1993**, *60*, 215−222.
(7) (a) Kitani, A.; Yano, J.; Sasaki, K. *J. Electroanal. Chem.* **1986**, *209*, 227. (b) Jelle, B. P.; Hagen, G. *J. Electrochem. Soc.* **1993**, *140*, 3560−3564.
(8) Duke, C. B.; Gibson, H. W. *Encyclopedia of Chemical Technology*; Kirk-Othmer: John Wiley: New York, 1982; Vol. 18, p 755.
(9) *Mod. Plast. Int.* **1982**, *12*, 46.
(10) Shinohara, H.; Chiba, T.; Aizawa, M. *Sensors Actuators* **1988**, *13*, 79.
(11) (a) Leclerc, M.; Guay, J.; Dao, L. H. *Macromolecules* **1982**, *22*, 649. (b) Wei, Y.; Focke, W. W.; Wnek, G. E.; Ray, A.; MacDiarmid, A. G. *J. Phys. Chem.* **1989**, *93*, 495. (c) MaCinnes, D., Jr.; Funt, B. L. *Synth. Met.* **1989**, *25*, 235. (d) Mattoso, L. H. C.; Mello, S. V.; Riul, A., Jr.; Oliverira, O. N., Jr.; Faria, R. M. *Thin Solid Film* **1994**, *244*, 714−717.
(12) (a) Yue, J.; Epstein, A. J. *J. Am. Chem. Soc.* **1990**, *112*, 2800. (b) Yue, J.; Wang, Z. F.; Cromack, K. R.; Epstein, A. J.; MacDiarmid, A. G. *J. Am. Chem. Soc.* **1991**, *113*, 2665. (c) Chen, S.-A.; Hwang, G.-W. *J. Am. Chem. Soc.* **1994**, *116*, 7939.
(13) Cao, Y.; Smith, P.; Heeger, A. J. *Synth. Met.* **1992**, *48*, 91.
(14) Chan, H. S. O.; Ng, S. C.; Sim, W. S.; Tan, K. L.; Tan, B. G. T. *Macromolecules* **1992**, *25*, 6029−6034.
(15) Cameron, R. E.; Clement, S. K. U.S. Patent 5,008,041, **1991**.
(16) Chan, H. S. O.; Gan, L. M.; Chew, C. H.; Ma, L.; Seow, S. H. *J. Mater. Chem.* **1993**, *3*, 1109−1115.
(17) Angelopoulos, M.; Patel, N.; Shaw, J. M. Electrical, Optical, and Magnetic Properties of Organic Solid State Materials; Materials Research Society Symposium Proceedings; Materials Research Society: Pittsburgh, **1994**, Vol. *328*, pp 173−178.

0002-7863/95/1517-8517$09.00/0

decomposition found in commodity thermoplastics, commercial exploitation of polyaniline has also been hampered by the low stability of HCl, the most commonly used dopant for polyaniline, especially at elevated temperatures and in a humid environment.[18] Slow evolution of corrosive HCl is unacceptable as it can cause damage to equipment and pose a health hazard. It has been shown that phosphonic acid doped emeraldine salts demonstrate a superior thermal stability without loss of volatile dopant species.[19] In this paper, we report a new self-doping emeraldine polymer derived from *o*-aminobenzylphosphonic acid. The polymer is characterized by elemental analysis, conductivity measurements, FTIR, UV−vis, X-ray photoelectron spectroscopy, X-ray powder diffraction, and $^{31}P\{^1H\}$ NMR to elucidate its structural and electronic properties. Studies of the pH dependence of its conductivity are also undertaken. A series of sodium salts of the polymer made by progressive neutralization of the phosphonic acid functions with sodium hydroxide has also been prepared to study the effects of Na^+ ion incorporation on its properties and to aid in spectral analyses and assignments. These systems represent the first structurally well-defined polyaniline ionomers, prepared from a presynthesized phosphonic acid functionalized aniline, that are intrinsically self-doped and water-soluble in the conducting form. Comparisons are made with other self-doping and water-soluble polyanilines prepared by the post treatment of the polyaniline base.[12]

Experimental Section

General Procedures. ^1H NMR spectra were recorded at 300 MHz on a Bruker ACF 300FT-NMR spectrometer using tetramethylsilane (TMS) or sodium 3-(trimethylsilyl)-1-propanesulfonate (DSS) as an internal reference. ^{13}C resonances were recorded at 125 MHz on a Bruker AMX 500FT-NMR spectrometer using the above mentioned references and reporting in ppm downfield from TMS. ^{31}P NMR were observed at 122 MHz on the Bruker ACF 300FT-NMR spectrometer with wideband proton decoupling using 85% H_3PO_4 as an external reference. Elemental analyses were performed by the Microanalytical Laboratory in our Department, using a Perkin-Elmer 240-C C,H,N analyzer for C, H, and N determinations and Plasmascan 700 Inductively-coupled Plasma analyzer for Cl, P, and Na determinations. Oxygen was calculated by difference. Vibrational (FTIR) spectra were recorded on a Perkin-Elmer 1725X FTIR spectrometer with 2-cm^{-1} resolution. Electronic spectra were acquired on a Hewlett Packard 8452A diode array spectrometer with 2-nm resolution. Second-order derivative spectra were used to identify λ_{max}. In some cases, extension of the optical spectra to 1000 nm (NIR) was achieved on a Perkin-Elmer UV-Vis-NIR Lambda 9 double-beam spectrometer. All reagents were prepared according to published procedures or were available from commercial sources and were used without further purification. Preparative flash chromatography was performed on Merck Silica Gel 60 (230−400 mesh).

Monomer Synthesis. *o*-Aminobenzylphosphonic acid monomer was synthesized in our laboratory according to Scheme 1.

Diethyl *o*-Nitrobenzylphosphonate (2). The Michealis-Arbusov reaction was employed. Triethyl phosphite (24.0 mL, 140 mmol) was placed with *o*-methylnitrobenzene **1** (27.0 g, 125 mmol) in a 100-mL round-bottomed flask equipped with a Dean-Stark condenser. The stirred mixture was heated to 110 °C (bath temperature) in an oil bath, at which point the reaction mixture turned brown and rapidly evolved bromoethane. After 2 min, the reaction was quenched by immersing the flask in an ice bath. *CAUTION:* Longer heating time led to fuming and degradation of the product. Unreacted triethyl phosphite was then removed *in vacuo* to give the crude material which was purified by flash chromatography (silica gel; chloroform) to afford 21.9 g (64%) of the title compound as a red-brown liquid: FTIR (neat) 3069, 2985, 2933, 2910, 1611, 1529, 1483, 1446, 1393, 1353, 1265, 1164, 1028, 972, 788, 700, 534 cm^{-1}.

Scheme 1. Synthetic Route to *o*-Aminobenzylphosphonic Acid

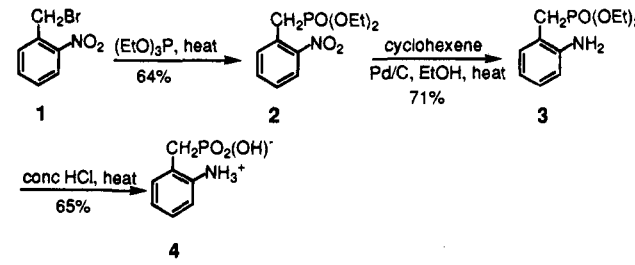

Diethyl *o*-Aminobenzylphosphonate (3). To a mixture of palladium on carbon (50 g, 5% Pd) and cyclohexene (24 mL, 430 mmol) in absolute ethanol (50 mL) was added a solution of **2** (19.4 g, 70 mmol) dissolved in 50 mL of absolute ethanol, and the mixture was heated, with stirring, under N_2 to reflux for 30 min until the disappearance of the $\nu(NO_2)$ frequencies by FTIR analysis. The mixture was cooled to room temperature and filtered to recover the Pd/C residue, which was washed repeatedly with ethanol. The combined filtrate was concentrated *in vacuo* to give a cloudy brown liquid. This was purified by ion-exchange (Dowex 50W-X8(H), 100−200 mesh) to afford 12.2 g (71%) of the title compound as a brown liquid: FTIR (neat) 3354, 3246, 2983, 2932, 2908, 1636, 1604, 1584, 1499, 1458, 1392, 1369, 1228, 1163, 1098, 1027, 970, 806, 752, 516 cm^{-1}; ^1H NMR (300 MHz, $CDCl_3$) δ 7.07−7.01 (m, 2H), 6.76−6.70 (m, 2H), 4.08−3.95 (m, 4H), 3.5 (br, 2H) 3.12 (d, J = 20.8 Hz, 2H), 1.25 (t, J = 7.1 Hz, 3H); ^{13}C NMR (125 MHz, $CDCl_3$) δ 146.0, 131.6 (d, J = 6.4 Hz), 128.2, 119.1, 117.3, 117.2, 62.4 (d, J = 6.4 Hz), 30.6 (d, J = 139 Hz), 16.4 (d, J = 5.3 Hz); ^{31}P NMR (122 MHz, $CDCl_3$) δ 27.7.

***o*-Aminobenzylphosphonic Acid (4).** Compound **3** (12.0 g, 49 mmol) was added to 12 M HCl (30 mL), and the mixture was heated to reflux for 6 h to give a cloudy brown solution. Activated carbon (1 g) was added and the mixture was refluxed for an additional 5 min. The reaction was allowed to cool to room temperature and filtered, and the filtrate was concentrated *in vacuo* to give a dark brown liquid. The crude product was recrystallized from hot water to afford 6.0 g (65%) of the title compound as a white solid: mp 268 °C dec; FTIR (KBr), 2756, 2590, 2192, 1653, 1536, 1497, 1464, 1414, 1244, 1186, 1139, 1101, 1062, 1005, 928, 856, 828, 773, 745, 562 cm^{-1}; ^1H NMR (300 MHz, D_2O) δ 7.38−7.33 (m, 4H), 3.12 (d, J = 20.0 Hz, 2H); ^{13}C NMR (125 MHz, D_2O) δ 134.9, 132.6, 131.6, 130.7, 126.0, 34.9 (d, J = 125.5 Hz); ^{31}P NMR (122 MHz, D_2O) δ 20.1; $\lambda(H_2O)$ = 206, 234 (sh), 284 nm. Anal. Calcd for $C_7H_{10}NO_3P$: C, 44.9; H, 5.4; N, 7.5. Found: C, 44.7; H, 5.3; N, 7.4.

Polymer Synthesis. The parent self-doping polymer **5** was synthesized by oxidative coupling of **4** in an acidic medium, based on modified procedures for polyaniline.[20] Its sodium salts **6**, **7**, and **8** were then obtained by progressive neutralization of the phosphonic acid functions with sodium hydroxide. Preparations of these polymers are given in Scheme 3.

Polymer 5. A pale-yellow solution of **4** (1.85 g, 9.9 mmol) dissolved in 3.5 M HCl (28 mL) was chilled to 0 °C in an ice-bath. A solution of sodium persulfate (2.40 g, 9.9 mmol) in deionized H_2O (20 mL) was added dropwise to this monomer-acid solution over a period of 4 h. The polymerization mixture was stirred and maintained at 0−5 °C in an ice-bath throughout. pH of the reaction medium was less than 1. The mixture was further allowed to stand overnight (16 h) at 0−5 °C, after which the precipitated polymer particles were filtered and rinsed with 2 M HCl (20 mL). The filter-cake was then carefully eluted with sufficient deionized water (200 mL) for 3 h on a Hirsch funnel until the eluate gave negative silver nitrate test and returned to the original pH of *ca.* 5.3. Subsequent vacuum drying for 16 h at room temperature gave 0.55 g (30%) of **5** as a dark green powder: FTIR (KBr) 3422, 3244, 3059, 2925, 2850, 1579, 1489, 1328, 1294, 1272, 1228, 1139,

(18) Uvdal, K.; Hansan, M. A.; Nilsson, J. O.; Salaneck, W. R.; Lungstroem, I.; MacDiarmid, A. G.; Ray, A.; Angelopoulos, A. *Springer Ser. Solid-State Sci.* **1987**, *76*, 262.

(19) Chan, H. S. O.; Ng, S. C.; Ho, P. K. H. *Macromolecules* **1994**, *27*, 2159−2164.

(20) Cao, Y.; Andreatta, A.; Heeger, A. J.; Smith, P. *Polymer* **1989**, *30*, 2305.

Scheme 2. Idealized Polaronic Representations of Polymers **5**–**8**

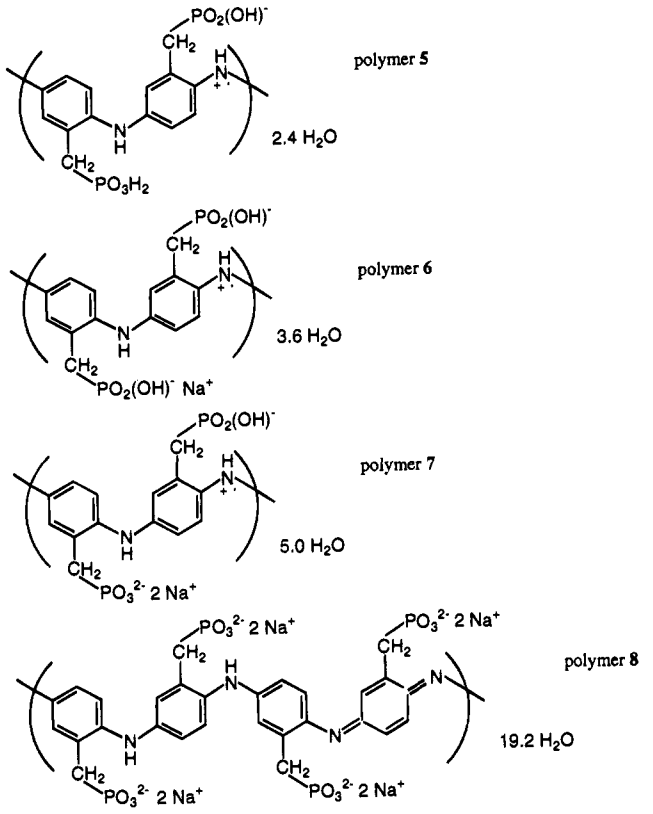

1056, 933, 811, 767, 511 cm^{-1}. Anal. Calcd for $(C_7H_{6.5}NO_3P)_n(H_2O)_{1.2n}$: C, 40.8; H, 4.8; N, 6.8. Found: C, 40.9; H, 4.9; N, 6.9; P, 13.6.

Polymer 6. To a test tube containing **5** (100 mg) was added stoichiometric amounts of 0.115 M sodium hydroxide to give a ratio of 0.50 mol of NaOH per mol of PO_3. The resultant polymer was completely soluble in the volume of base used to give an intense green solution. Gradual removal of water over phosphorus pentoxide in a vacuum desiccator back-flushed with N_2 (*ca.* 30 mmHg) afforded **6** as a black hygroscopic solid after 30 h: FTIR (KBr) 3419, 3244, 2919, 2850, 1571, 1479, 1326, 1293, 1268, 1222, 1131, 1048, 904, 810, 767, 508 cm^{-1}; ^{13}C NMR (125 MHz, D_2O) δ 156–115 (br m), 37–30 (br); ^{31}P NMR (122 MHz, D_2O) δ 28–10 (br); $\lambda(H_2O)$ = 310, 436, 556, 890 (sh), 974 nm. Anal. Calcd for $(C_7H_7NO_3PNa_{0.5})_n(H_2O)_{1.8n}$: C, 36.9; H, 4.7; N, 6.1; Na, 5.0. Found: C, 36.9; H, 4.7; N, 6.1; Na, 5.2.

Polymer 7. **7** was made analogously using a stoichiometry of 1.0 mol of NaOH per mol of PO_3 to afford another black hygroscopic solid: FTIR (KBr) 3422, 3244, 2919, 2850, 1597, 1482, 1324, 1294, 1268, 1231, 1135, 1053, 965, 903, 769, 514 cm^{-1}; ^{1}H NMR (300 MHz, D_2O) δ 8.0–6.4 (br, 3H), 3.2–2.7 (br, 2H); ^{31}P NMR (122 MHz, D_2O) δ 25–14 (br m); $\lambda(H_2O)$ = 316, 436, 558, 890 (sh), 973 nm; λ(thin film) = 306, 420, 606 nm. Anal. Calcd for $(C_7H_{6.5}NO_3PNa)_n(H_2O)_{2.5n}$: C, 33.4; H, 4.6; N, 5.6; Na, 9.1. Found: C, 34.0; H, 5.0; N, 5.6; Na, 8.6.

Polymer 8. **8** was obtained similarly using a ratio of 2.0 mol of NaOH per mol of PO_3. The black solid formed was extremely hygroscopic: FTIR (KBr) 3422, 2919, 2850, 1633, 1497, 1314, 1233, 1144, 1058, 970, 715, 531 cm^{-1}; ^{1}H NMR (300 MHz, D_2O) δ 7.5–6.6 (br m, 3H), 2.8 (br s, 2H); ^{13}C NMR (125 MHz, D_2O) δ 146–116 (br m), 38–36 (br); ^{31}P NMR (122 MHz, D_2O) δ 19.0, 18.6; $\lambda(H_2O)$ = 308, 424, 546, 966 nm; λ(thin film) = 300, 434, 584 nm. Anal. Calcd for $(C_7H_{5.5}NO_3PNa_2)_n(H_2O)_{4.8n}$: C, 26.9; H, 4.8; N, 4.4; Na, 14.6. Found: C, 26.5; H, 4.8; N, 4.2; Na, 12.9.

Polymer 9. **5** (200 mg) was re-equilibrated in 2 M HCl (500 mL) for 6 h followed by filtration and vacuum-drying (16 h, 25 °C) to afford **9** as a dark-green solid. Equilibrium pH was *ca.* 0.0. Analysis showed **9** to be essentially identical to **5**. FTIR (KBr) 3423, 3244, 3059, 2925, 2850, 1579, 1489, 1328, 1294, 1272, 1228, 1139, 1056, 933, 811, 767, 511 cm^{-1}. Anal. Calcd for $(C_7H_{6.5}NO_3P)_n(H_2O)_{1.1n}(HCl)_{0.2n}$: C, 39.9; H, 4.3; N, 6.6. Found: C, 40.3; H, 4.8; N, 6.4.

Scheme 3. Synthetic Route to Polymers **5**–**8**

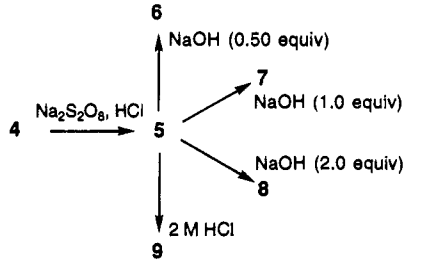

X-ray Photoelectron Spectroscopy. X-ray photoelectron spectroscopy (XPS) experiments were performed on a VG ESCA/SIMS LAB MKII spectrometer using a Mg Kα (1253.6 eV) source. Core-level spectra were acquired on vaccum-dried polymer powders (**5** and **9**) mounted on standard sample holders by double-sided adhesive tape, or films (**6**, **7** and **8**) cast directly onto the metal holders. After linear background subtraction, N1s and O1s spectra were fitted with Gaussian component peaks allowing slight variations in the full-width at half-maximum (fwhm) to reflect their chemical-state dependence.[21] Binding energies (BE) were referenced to the maxima in the smoothed C1s envelopes, defined at 285.0 eV,[21] to compensate for surface-charging. Surface atomic stoichiometries were obtained from peak areas corrected with experimental sensitivity factors and are expected to have a ±10% error.

X-ray Diffraction. X-ray diffraction (XRD) powder patterns for the polymers were obtained on a Philips X-ray diffractometer using a Cu Kα (1.54A) X-ray source with Ni filter. The powders were mounted by double-sided adhesive tape on glass sample holders and 2θ scanned at 2° deg min^{-1}.

DC Conductivity and Its pH Dependence. DC conductivity of the polymers was measured on compacted pellets using the four-point probe method. Its pH dependence was determined by equilibrating finely-powdered **5** (200 mg) with HCl solutions (500 mL) of various strengths for 6 h. The polymer was then recovered by filtration and dried under vacuum (16 h, 25 °C) before being compacted into a pellet for measurements. Final equilibrium pH values of 0.0, 1.0, 2.7, and 5.3 (deionized H_2O) were studied. Extension to the basic pH range failed because of the solubility of **5** in ammonia solution.

Cyclic Voltammetry. Cyclic voltammetry studies of the polymer were performed on a EG&G 273 Potentiostat/Galvanostat using EG&G 270/250 Research Electrochemical Software 4.0. The single-compartment electrochemical cell was equipped with a platinum foil working electrode (0.5 cm^2), a saturated calomel electrode (SCE), and a platinum wire counter electrode. A thin polymer film was cast onto the working electrode by evaporation from an aqueous solution of **6** in a vacuum desiccator (*ca.* 30 mmHg), followed by treatment with HCl fumes to render it water-insoluble. Steady-state multicycle switching response was obtained on a sweep rate of 50 mV s^{-1}, after pre-conditioning with at least 20 cycles (15 min). pH dependence was investigated in HCl/NaCl solutions of constant ionic strength over the pH range of −0.0 to 2.1. All emf values are reported *vs* SCE.

Results and Discussion

General Considerations. The idealized polaronic forms[22] of polymers **5**–**8** are given in Scheme 2. Elemental analysis, spectroscopic results (FTIR, UV–vis, ^{31}P NMR, and XPS), and cyclic voltammetry are consistent with the para head-to-tail coupling of *o*-aminobenzylphosphonic acid monomer to give a substituted polyaniline **5** in the emeraldine oxidation state.[23] Simultaneous proton transfer from the phosphonic acid functions to about half the nitrogen atoms directly gives the self-doped

(21) Beamson, G.; Briggs, D. *High Resolution XPS of Organic Polymers: The Scienta ESCA Database*; John Wiley and Sons: Chichester, England, 1992.

(22) MacDiarmid, A. G.; Chiang, J. C.; Richter, A. F.; Epstein, A. J. *Synth. Met.* **1987**, *18*, 285.

(23) Wang, Z. H.; Javadi, H. H. S.; Epstein, A. J.; Ray, A.; MacDiarmid, A. G. *Phys. Rev. B* **1990**, *42*, 5411.

Table 1. Bulk Atomic Compsiton, Surface Atomic Composition, and dc Conductivity (σ) of Polymers **5**–**9**

polymer	bulk atomic ratio (surface atomic ratio)	σ, S cm^{-1}
5	$C_{7.0}H_{10.0}N_{1.0}P_{0.9}O_{4.2}Cl_{0.05}$ ($C_{7.7}N_{1.0}P_{1.0}O_{3.2}$)	1.5×10^{-3}
6	$C_{7.0}H_{10.7}N_{1.0}P_{0.9}O_{4.9}Na_{0.5}Cl_{0.05}$ ($C_{7.6}N_{1.0}P_{1.0}O_{3.5}$)	0.6×10^{-3}
7	$C_{7.0}H_{12.3}N_{1.0}P_{1.0}O_{5.3}Na_{0.9}Cl_{0.05}$ ($C_{8.1}N_{1.0}P_{1.0}O_{4.6}$)	0.08×10^{-3}
8	$C_{7.0}H_{15.2}N_{1.0}P_{0.9}O_{8.3}Na_{1.8}Cl_{0.05}$ ($C_{9.8}N_{1.0}P_{0.8}O_{4.7}$)	1×10^{-7}
9	$C_{7.0}H_{9.9}N_{1.0}P_{0.9}O_{4.0}Cl_{0.2}$ ($C_{9.0}N_{1.0}P_{1.0}O_{3.5}Cl_{0.15}$)	1.0×10^{-3}

polyzwitterionic form. Stepwise compensation with NaOH progressively neutralizes the excess phosphonic acid functions to give first a hemisodium polymer **6**, then a monosodium polymer **7**, and finally a disodium polymer **8**. **8** corresponds essentially to the undoped insulating form[23] of polyaniline. Redoping of **5** with HCl substitutes some Cl^- for phosphonate counterions but has no effect on the polymer's electrical conductivity.

Bulk atomic ratios (microanalysis), surface atomic ratios (XPS), and conductivities (σ) of the polymers are presented in Table 1. A maximum conductivity of 1×10^{-3} S cm^{-1} is exhibited by **5** and **9**. Electrical conductivity of the emeraldine polymers has a marked sigmoidal dependence on the pH of the medium.[24] In contrast, this self-doped **5** does not exhibit any conductivity dependence on pH below 6. σ values remain essentially constant at $(1.1 \pm 0.3) \times 10^{-3}$ S cm^{-1} over the pH range from 0 to 6. Similar observations have been reported for sulfonated polyaniline.[12b]

5 is insoluble in common organic solvents, water, or concentrated H_2SO_4, but soluble in dilute (>20 mM) NH_3 to give an intense green solution owing to partial deprotonation of excess PO_3H_2 functions to form an ionomer that interacts strongly with H_2O. **6**, **7**, and **8** are also insoluble in common organic solvents, but freely soluble in H_2O (up to 10 wt % for **6**, >3 wt % for **7** and **8**) to give intense green solutions (**6** and **7**) and blue-violet solutions (**8**) from which films can be cast. Using SEM at 5000× magnification the film morphologies have been found to be smooth, structureless, and non-porous. Very dilute solutions of **6** and **7** deprotonate slowly to **8** when the medium is insufficiently acidic.

Powder XRD reveals these polymers to be predominantly amorphous with no well-defined Bragg reflections that can be associated with long-range structural order. Only a broad featureless hump centred at $2\theta = 23.5°$ could be detected. This can be related to steric hindrance of the bulky methanephosphonate groups preventing the formation of close-packed crystalline regions.

X-ray Photoelectron Spectroscopy. The N1s core level spectra (Figure 1) are fitted with three components[25] corresponding to neutral amine or imine sites at 399.6 eV and protonated, positively-charged N sites at 401.0 and 402.5 eV. The identities of the two higher BE components are still under debate. Various authors have assigned them to charged-N sites in variable valence field of the counterions,[25e] protonated imine- and amine-N,[25a,d] or polaronic- and bipolaronic-N.[25c] Nonetheless, the total area of both these components corresponds well to the amount of counteranions intercalated[14,25a,d] and hence the N-doping level—the fraction of protonated N sites in the polymer—can be evaluated (see Table 2). It is found that **5** and **9** are doped to 43% and 40%, repectively. The presence of a strongly acidic $-CH_2PO_3H_2$ function on every ring has not resulted in further protonation of the polymer beyond the emeraldine salt form. Neither can further doping be achieved through re-equilibration of **5** in strong HCl. This indicates that maximum protonation has been achieved in the polyzwitterion and reaffirms the particular stability conferred by the emeraldine salt electronic structure. **6**, **7**, and **8** show the expected decrease in doping level and conductivity with increasing NaOH compensation. Despite favorable doping levels in **5**, **6**, **7**, and **9**, the conductivity is some three orders of magnitude lower than conventional acid-doped polyanilines. This may be attributed to (i) steric reduction of chain coherence and increase in chain

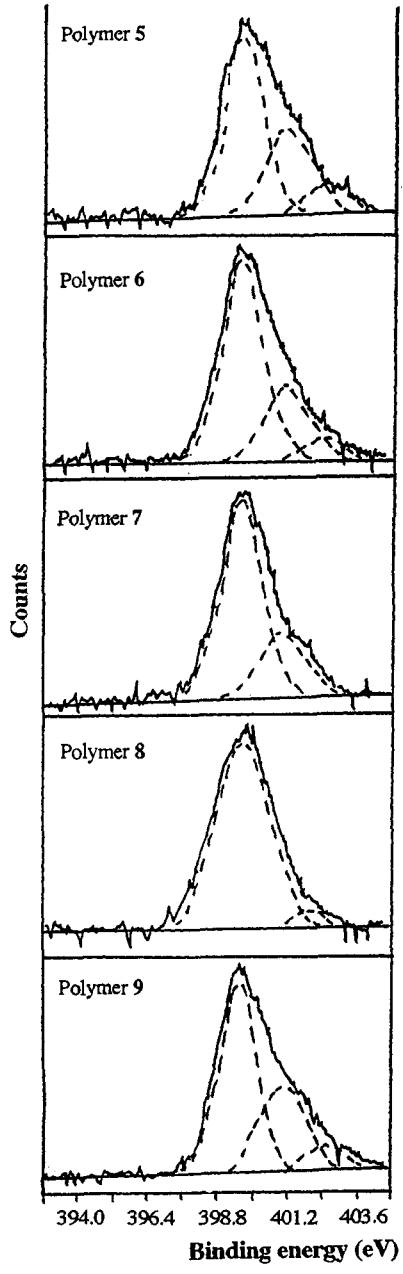

Figure 1. Curve-resolved XPS N1s spectra of polymers **5**–**9**.

(24) (a) MacDiarmid, A. G; Chiang, J. C.; Halpern, M.; Huang, W. S.; Mu, S. L.; Somasiri, N. L. D.; Wu, W.; Yaniger, S. I. *Mol. Cryst. Liq. Cryst.* **1985**, *121*, 173. (b) Chiang, J. C.; MacDiarmid, A. G. *Synth. Met.* **1986**, *13*, 193. (c) Salaneck, W. R.; Lundstrom, I.; Hjertberg, T.; Duke, C. B.; Conwell, E.; Paton, A.; MacDiarmid, A. G.; Somasiri, N. L. D.; Huang, W. S.; Richter, A. F. *Synth. Met.* **1987**, *18*, 291.

(25) (a) Tan, K. L.; Tan, B. T. G.; Kang, E. T.; Neoh, K. G. *Phys. Rev. B* **1989**, *39*, 8070. (b) Ray, A.; Richter, A. F.; MacDiarmid, A. G.; Epstein, A. J. *Synth. Met.* **1989**, *29*, E151. (c) Kumar, S. N.; Gaillard, F.; Bouyssoux, G. *Synth. Met.* **1990**, *36*, 111. (d) Chan, H. S. O.; Ho, P. K. H.; Tan, K. L.; Tan, B. T. G. *Synth. Met.* **1990**, *35*, 333. (e) Yue, J.; Epstein, A. J. *Macromolecules* **1991**, *24*, 4441. (f) Chan, H. S. O.; Ng, S. C.; Sim, W. S.; Seow, S. H.; Tan, K. L.; Tan, B. T. G. *Macromolecules* **1993**, *26*, 144.

Table 2. Curve-Resolved N1s and O1s Core Levels and dc Conductivity (σ) of Polymers **5**–**9**

	N1s area ratios, %				O1s area ratios, %					
polymer	~399.7	~401.1	~402.6	N^+/N, %	~531.2	~531.5	~532.8	~534.6	P^-/P, %	σ, S cm^{-1}
5	58	32	11	43	26	18	50	6	42	1.5×10^{-3}
6	65	27	7	34	43	5	47	5	81	0.6×10^{-3}
7	74	26	0	26						0.08×10^{-3}
8	96	5	0	5						1.0×10^{-7}
9	60	31	9	40	20	18	52	11	34	1.0×10^{-3}

free-volume caused by the pendent groups, (ii) increased concentration of defects, such as $^+NH_2$, and (iii) increased charge-pinning on the nitrogen sites through strong hydrogen bonding between $-PO_2(OH)^-$ and NH^+ as shown below:

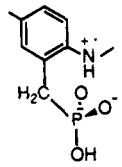

The strong Coulombic attraction—substantiated also by other spectroscopic evidence to be presented later—causes the positive charge, either polaronic or bipolaronic, to be effectively trapped on the nitrogen atom. Such localization effects have been observed in EPR experiments[26] and also in sulfonated polyaniline. Thermopower studies have found an effective localization length $a_{\|}^{-1} = 0.6$ nm in that polymer,[12b] in contrast to $a_{\|}^{-1} = 3$ nm for polyaniline–HCl.[27] All three factors lead to enhanced inter- and intra-chain spin diffusion barrier which hinders the quasi-one-dimensional variable range hopping conduction mechanism.[22,27]

O1s core level spectra and data are presented in Figure 2 and Table 2, respectively. Although the BE shifts in this element are typically small and assignments not always unambiguous,[21,28] the use of appropriate model compounds (benzylphosphonic acid and *o*-aminobenzylphosphonic acid) allows the O1s envelopes of **5**, **6**, and **9** to be fitted to a consistent set of spectral parameters. The curve-fitted phosphonate oxygens[19] are $^{-1/2}O-P-O^{-1/2}$ at 531.2 eV (fwhm 1.85 eV), P=O at 531.5 eV (fwhm 1.75 eV), and P–OH at 532.8 eV (fwhm 1.75 eV). The 531.5-eV component has been fitted into the spectra to achieve an internally consistent P=O stoichiometry. The total area of the deconvoluted phosphonate oxygens correlates well to the 3:1 ratio with P2p areas after sensitivity corrections. The ratio of singly-ionized phosphonates to total phosphonic acid (P^-/P) may thus be determined (Table 2) and compared with the level of N doping to elucidate the doping mechanism. For **5**, the 43% nitrogen doping arises solely via internal proton transfer from the phosphonic acid groups. Treatment with NaOH to generate **6** preferentially removes the more acidic phosphonic acid protons. Phosphonic acid ionization increases 39% while nitrogen protonation falls only 9%. Thus, this material is still 34% self-doped. Even with half-neutralization as in the monosodium polymer **7**, 26% self-doping is still retained. On the other hand, re-equilibration of **5** with HCl leads to only 6% HCl-doping (not shown) and leaving 34% self-doping. These results allude to the high stability of the *self-doped* emeraldine salt. In both **6** and **9**, the 532.8-eV component also receives contribution from H_2O[28] present in the polymer matrix. For all three spectra, a fourth component at 534.6 eV (fwhm 1.9 eV) is necessary to complete the deconvolution. Such a high BE is typical of H_2O species associated with a positive charge.[19,28] In the present study, this probably arises from H_2O molecules hydrogen bonded to positively-charged NH^+ sites. Supporting evidence is provided by thermogravimetry studies, which show a large H_2O desorption step extending up to 150

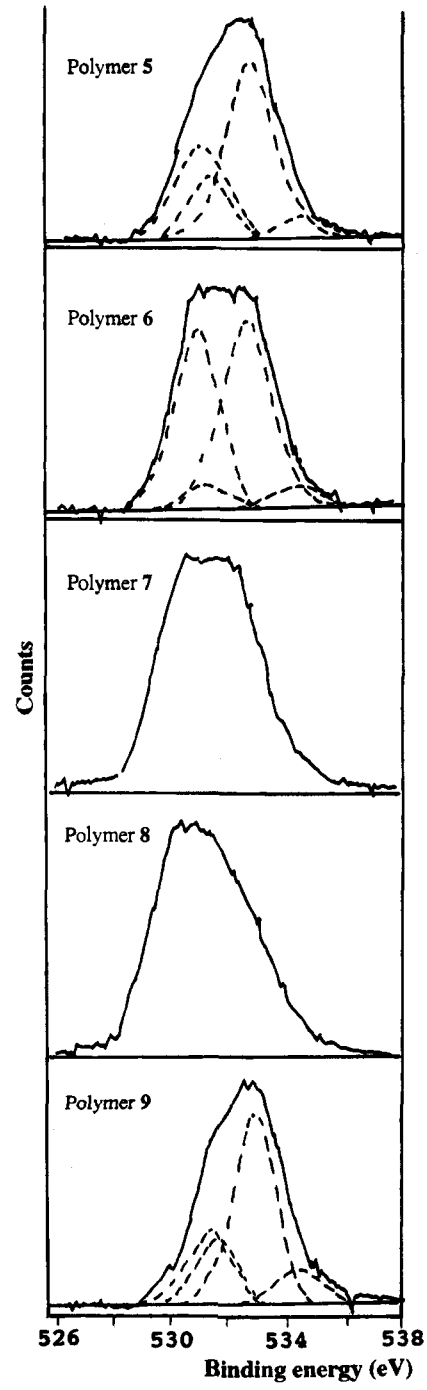

Figure 2. XPS O1s spectra of polymers **5**–**9**. Some of the spectra have been fitted with Gaussian components (refer to text).

(26) Lapkowski, M.; Genies, G. M. *J. Electroanal. Chem.* **1990**, *279*, 157.
(27) Epstein, A. J.; MacDiarmid, A. G. *Synth. Met.* **1991**, *41*, 601.
(28) *Handbook of X-ray Photoelectron Spectroscopy*; Chastain, J., Ed.; Perkin-Elmer Corp.; Physical Electronics Division: Minnesota, 1992.

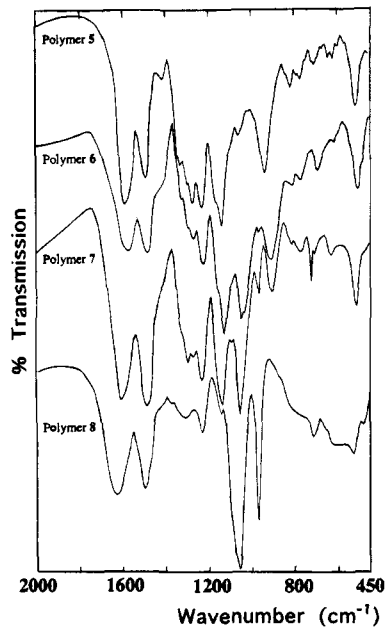

Figure 3. Baseline corrected FTIR spectra of polymers **5**–**8** showing the 1800–450-cm^{-1} region.

°C, and FTIR, which shows strong ν(O–H) frequencies at 3422 cm^{-1}. More extensive NaOH compensation in **7** and **8** introduces doubly-ionized PO_3^{2-} in addition to $PO_2(OH)^-$ and OH^-, making curve-fitting impossible. Overall, the entire O1s envelope shifts to lower BE, consistent with increasing participation of PO_3^{2-} and disappearance of H_2O hydrogen bonded to positive sites.

Fourier-Transformed Infrared Spectroscopy. The baseline-adjusted FTIR spectra of polymers **5**–**8** are compared in Figure 3. The 1580 to 1480-cm^{-1} band intensity ratio is consistent with a predominant emeraldine oxidation state.[29] With increasing base compensation, the 1580-cm^{-1} band shifts toward higher frequency, reaching 1633 cm^{-1} in **8**, in agreement with the decline in nitrogen protonation.

However, our polymers absorb differently from other emeraldine salts in the 1350–1230-cm^{-1} ν(Ph–N) spectral region. The latter shows only two bands[31] at 1300 and 1245 cm^{-1} whereas ours give four. The first pair of bands at 1294 and 1228 cm^{-1} can be assigned to essentially unperturbed Ph–NH–Ph stretching frequencies, while the pair at 1328 and 1272 cm^{-1} receives contribution from mechanical coupling to the hydrogen-bonded $CH_2PO_2(OH)^-$. With increasing NaOH compensation, the second pair falls in relative intensity, consistent with decreasing amounts of NH^+ in the polymers. Severe decline in the oscillator strength of these bands occurs in **8** and is related to the loss of dipolar character[29a] and increased symmetry in the Ph–N–Ph bonds with deprotonation.

FTIR confirms the progressive ionization of $-PO_3H_2$ functions with increasing base compensation. PO_2^- vibrations[30] at *ca.* 1135 cm^{-1} are found in decreasing intensity across **5**, **6**, and **7**, whereas PO_3^{2-} vibrations (ν_{as} and ν_s)[30] at 1053 and 965 cm^{-1} first appear in **7** but dominate the spectrum of **8**. Futhermore, the band at *ca.* 1135 cm^{-1} is sensitive to the nature of countercations[30] and could thus provide structural information on the ionic domains in these polymers. In particular, the shift in this band by -8 cm^{-1} on going to **6** and then $+5$ cm^{-1} on going to **7** indicates that $PO_2(OH)^-$ domains in **7** are largely associated with NH^+ rather than Na^+. Therefore, the PO_3^{2-} domains must be counterbalanced by Na^+.

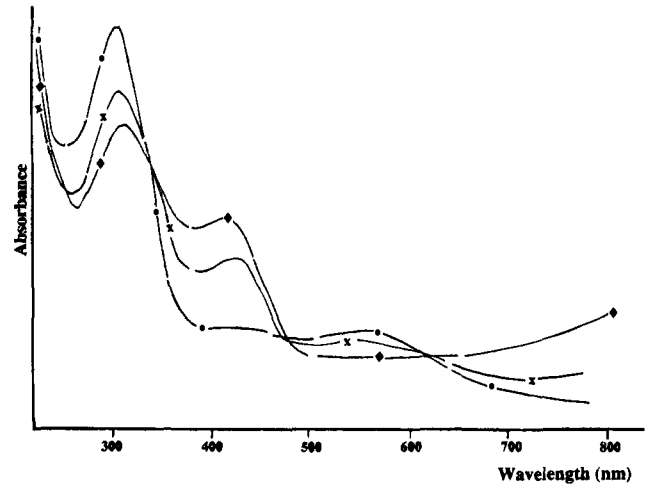

Figure 4. UV–vis spectra of polymers (a) **6** (◆), **7** (×), and **8** (●), measured on freshly-prepared 10^{-4} M aqueous solutions.

Ultraviolet–Visible Spectroscopy. The electronic spectra of aqueous polymer solutions are shown in Figure 4. All three polymers show electronic transitions at 3.98, 2.24, 2.85, *ca.* 1.4, and 1.28 eV. Both 3.98- and 2.24-eV bands undergo a hyperchromic shift on going from **6** to **8**. The 3.98-eV absorption has been attributed to $\pi_B \rightarrow \pi^*$ bandgap transition with other contributions.[31] Hypsochromic shift of this transition compared to conventional polyanilines (3.84 eV)[19,32] and sulfonated polyaniline (3.88 eV)[12b] could be ascribed to either a decrease in ring conjugation caused by a larger steric interference between the ortho substituent and neighboring ring hydrogens[12a,14,25f] or a significant hydrogen bond interaction between $PO_2(OH)^-$ and $NH^{\bullet+}$ leading to a increased participation of the nitrogen wave function in the HOMO and thereby widening of the low lying $\pi_B \rightarrow \pi_S$ gap. The 2.24-eV absorption has been assigned to $\pi_B \rightarrow \pi_Q$ exciton transition.[31] This band too is hypsochromically shifted from conventional polyanilines (2.03 eV),[19,32] but similar to sulfonated polyaniline.[12b] It may be caused by steric repulsion opening up the ring torsion angle[12b] and hence reducing overlap between the quinoid unit and the benzenoid unit.

Both the 2.85- and 1.4-eV absorptions are assigned to optical transitions of the metallic polaron band.[31,33,34] Unlike conventional polyanilines,[19,32] the 2.85-eV feature in our polymers shows considerable gain in oscillator strength and develops into a distinct peak. The difference may be related to charge-pinning effects. It is interesting to note that polymer **8** still retains some slight polaronic character because of residual protonation. Thin-film spectra (300–800 nm) of **7** and **8** solution cast on quartz substrates show similar features, indicating that (i) the conjugation lengths of the extended-coil conformation[35] in dilute aqueous solution are not much different from that in the solid state and (ii) the observed electronic features have an intra-chain rather than inter-chain origin.

(29) (a) Tang, J.; Jing, X.; Wang, B.; Wang, F. *Synth. Met.* **1988**, *24*, 231. (b) Harada, I.; Furukawa, Y.; Ueda, F. *Synth. Met.* **1989**, *29*, E303.

(30) Thomas, L. C. *The Identification of Functional Groups in Organophosphorus Compounds*; Academic Press: London, England, 1974.

(31) (a) Duke, C. B.; Paton, A.; Conwell, E. M.; Salaneck, W. R.; Lundstrom, I. *J. Chem. PHys.* **1987**, *86*, 344. (b) Stafstrom, S.; Sjogren, B. *Synth. Met.* **1989**, *29*, E219.

(32) Glarum, S. H.; Marshall, J. H. *J. Phys. Chem.* **1988**, *92*, 4210.

(33) Stafstrom, S.; Bredas, J. L.; Epstein, A. J.; Woo, H. S.; Tanner, D. B.; Huang, W. S.; MacDiarmid, A. G. *Phys. Rev. Lett.* **1987**, *59*, 1464.

(34) McCall, R. P.; Ginder, G. M.; Leng, J. M.; Ye, H. J.; Manohar, S. K.; Masters, J. G.; Asturias, G. E.; MacDiarmid, A. G.; Epstein, A. J. *Phys. Rev. B* **1990**, *41*, 5202.

(35) *Polyelectrolytes: Science and Engineering and Technology*; Hara, M., Ed.; Marcel Dekker Inc.: New York, 1993.

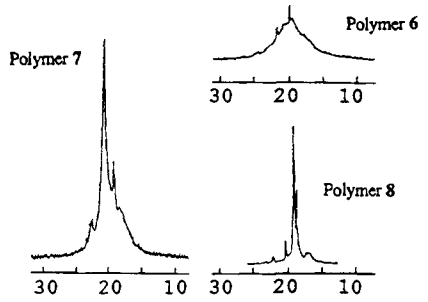

Figure 5. $^{31}P\{^1H\}$ NMR spectra of polymers **6**–**8**, measured at 122 MHz on 3 wt % aqueous solutions.

^{31}P Nuclear Magnetic Resonance. ^{31}P NMR spectra of D_2O solutions (3 wt %) of **6**, **7**, and **8** are compared in Figure 5. The observed chemical shifts (18–23 ppm) are consistent with the presence of singly- or doubly-ionized phosphonate moieties.[36] **8** exhibits the two most intense lines at 19.0 and 18.6 ppm. The line width (fwhm) of the stronger 19-ppm signal is 27 Hz. In contrast, **6** exhibits mainly a broad resonance at 20.1 ppm with a fwhm of 555Hz. **7** gives composite characteristics of sharp resonances at 20.9 and 19.3 ppm superimposed on a broad feature centered at *ca.* 19 ppm. These results accord with the presence of unpaired spins (polarons) in the protonated segments of the solvated polymers **6** and **7**. The narrow lines arise from ^{31}P nuclei in the unprotonated segments of the PANI chains, while the broad ones arise from ^{31}P nuclei interacting with spins in the protonated segments. Absence of any significant contact and pseudocontact[37] shifts in these resonances indicate the unpaired spin has an isotropic character and is neither delocalized nor spin-polarized onto the ^{31}P nuclei. Such spins are expected to reside predominantly on the N atoms[33,38] and, in solution, may either delocalize over several units or rapidly diffuse through the protonated chain segments. Hence, substantial line width broadening observed in **6** and in the 19-ppm line of **7** can be related to a hydrogen bond interaction between the PO_3 moiety and the NH radical, leading to an efficient dipolar relaxation mechanism[37] for the ^{31}P nuclei. Whereas delocalization or rapid spin diffusion results in a single, averaged ^{31}P signal in **6**, the protonated and unprotonated segments in **7** remain distinct on the NMR time scale, giving rise to a multiplet of signals.

Redox Properties. Figure 6 shows the effect of pH variations, at constant ionic strength,[39a] on the multicycle voltammogram of **5**. Different from other polyaniline systems which show two sets of redox peaks ($E_{1/2}$ = 0.18 and 0.74 V in the parent polyaniline[3b]), this polymer displays only one set of redox activity at $E_{1/2}$ = 0.39 V (1.0 M HCl) over the full potential window from −0.2 to 1.2 V. This pair of peaks shifts −59 mV/pH unit. The process is thus characteristic of one H^+ loss per electron loss and may be identical to the first redox wave in the parent polyanilines[3b,39] and sulfonated polyaniline.[12b] Absence of the second redox process suggests that our polymers

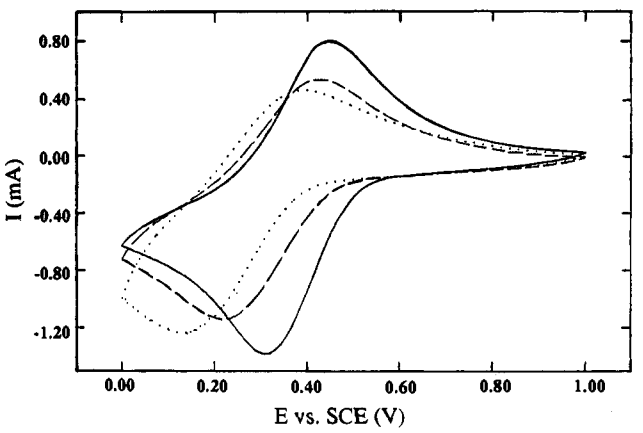

Figure 6. CV of polymer **5** on Pt foil at different pH: (a) —, 1.0 M HCl, pH = 0.0; (b) - - -, 0.10 M HCl + 0.90 M NaCl, pH = 1.1; (c) ···, 0.01 M HCl + 0.99 M NaCl, pH = 2.1. Scan rate, 50 mV s^{-1}.

in the emeraldine state are exceptionally resistant to oxidation to the pernigraniline[3] state. Repeated cycling between 0.0 and 1.0 V (100 cycles) does not result in substantial loss of electroactivity. In contrast, irreversible degradation occurs rapidly once the potential reaches 0.8 V in other reported polyanilines[12b,39] with a third set of redox peaks appearing between the original two. This stability may be related to the hydrogen bond stabilization of the emeraldine salt which is lost on going to the weakly basic pernigraniline[3] form. The higher $E_{1/2}$ for **5** as compared to the parent polyaniline and sulfonated polyaniline arises naturally from the lower chain conjugation in these polymers.

Conclusion

A novel conducting polyaniline has been synthesized by persulfate oxidative coupling of *o*-aminobenzylphosphonic acid in an acidic medium. XPS confirms the polymer is obtained directly in the 43% polyzwitterionic (i.e. self-doped) emeraldine form with internal proton transfer from the phosphonic acid functions to the nitrogen bases. Significant steric effects and charge-pinning in the hydrogen-bonded zwitterions are indicated. The self-doping persists up to significant levels of NaOH compensation, with 34% retention in the hemisodium and 26% retention in the monosodium material. FTIR provides evidence of strong intra-chain hydrogen bonding between the charged NH^+ and $PO_2(OH)^-$. Progressive base compensation results in stepwise ionization of the remaining phosphonic acid functions, until the fully-neutralized disodium polymer is in the undoped form. The half-neutralized monosodium polymer contains NH^+ domains that are counterbalanced by singly-ionized phosphonate moieties. UV–vis spectra of these polymers show polaronic features that are analogous to other emeraldine salts due to similar electronic structures, but different transition moments and energies due to perturbation effects of the polar phosphonate moieties. ^{31}P NMR indicates the existence of isotropic spins in the solvated self-doped polymer chains. Protonated and unprotonated segments of the monosodium polymer are distinct on the NMR time scale. In marked contrast to the acid-doped polyanilines, no oxidation to the pernigraniline form is possible under the conditions of the CV studies, alluding to the higher stability of the self-doped emeraldine structure. In summary, these partially-neutralized ionomers point the way to achieve intrinsically self-doped, conducting polymers that are water-processable in the conducting form.

JA950993E

(36) (a) Model compounds Na^+ *o*-$H_2NPhCH_2PO_3H^-$ and $2Na^+$ *o*-$H_2NPhCH_2PO_2^{2-}$ give ^{31}P resonance at 20.6 and 19.0 ppm, respectively, in D_2O. (b) *Phosphorus-31 NMR: Principles and Applications*; Gorenstein, D. G., Ed.; Academic Press Inc.: New York, 1984. (c) *Handbook of Phosphorus-31 Nuclear Magnetic Resonance Data*; Tebb, J. C., Ed.; CRC Press Inc.: Boca Raton, FL, 1991.

(37) (a) *NMR of Paramagnetic Molecules: Principles and Applications*; La Mar, G. N., Horrocks, W. D., Jr.; Holm, R. H., Eds.; Academic Press Inc.: New York, 1973. (b) Bertini, I., Luchinat, C. In *Physical Methods for Chemists*, 2nd ed.; Drago, R. S., Ed.; Saunders & College Publishing: Philadelphia, 1992; p 500.

(38) McCall, R. P.; Ginder, J. M.; Roe, M. G.; Asturias, G. E.; Scherr, E. M.; MacDiarmid, A. G.; Epstein, A. J. *Phys. Rev. B* **1989**, *39*, 10174.

(39) (a) Inzelt, G.; Horanyi, G. *Electrochim. Acta* **1990**, *35*, 27. (b) Kalaji, M.; Nyholm, L.; Peter, L. M. *J. Electroanal. Chem.* **1991**, *313*, 271.